Journal Name

ARTICLE

RAFT Dispersion Polymerization of Glycidyl Methacrylate for the Synthesis of Epoxy-Functional Block Copolymer Nanoparticles in Mineral Oil

Received 00th January 20xx,
Accepted 00th January 20xx

DOI: 10.1039/x0xx00000x

www.rsc.org/

Philip J. Docherty, Matthew J. Derry* and Steven P. Armes*

Epoxy-functional poly(stearyl methacrylate)-poly(glycidyl methacrylate) (PSMA-PGlyMA) diblock copolymer nanoparticles are synthesized via reversible addition-fragmentation chain transfer (RAFT) dispersion polymerization of glycidyl methacrylate (GlyMA) in mineral oil at 70 °C. This efficient polymerization-induced self-assembly (PISA) formulation yields well-defined spheres of tunable diameter as confirmed by dynamic light scattering (DLS) and transmission electron microscopy (TEM) studies. ^{1}H NMR spectroscopy and gel permeation chromatography (GPC) studies indicate that such non-polar dispersions exhibit greater stability during their long-term storage at 20 °C compared to related epoxy-functional nanoparticles prepared via RAFT aqueous emulsion polymerization. Model epoxy-amine ring-opening reactions using *N*-methylaniline demonstrate the potential for post-polymerization functionalization of such spherical nanoparticles.

Introduction

Since its inception, reversible addition-fragmentation chain transfer (RAFT) polymerization has enabled the synthesis of highly functional polymers of narrow molecular weight distribution and controlled architecture from a wide range of vinyl monomers.[1-3] As a result, such polymers have shown promise for biomedical applications,[4] personal care products[5] and oil viscosity modification.[6] For example, The Lubrizol Corporation utilized the versatility of RAFT polymerization to develop a series of commercially successful methacrylic star polymers (*Asteric*™) that exhibit enhanced control of lubricant rheology compared to the corresponding copolymer.[6]

Many research groups have explored RAFT-mediated polymerization-induced self-assembly (PISA)[7-10] as a highly convenient route to well-defined block copolymer nanoparticles in aqueous,[11-17] alcoholic[18-28] and non-polar[29-33] media. PISA involves using a solvophilic macromolecular chain transfer agent (macro-CTA) to polymerize a monomer that forms an insoluble polymer block, thus driving *in situ* self-assembly of the resulting block copolymer chains to form a range of nano-objects (most commonly spheres, worms or vesicles). Recently, various PISA formulations in non-polar media[8] have utilized oil-soluble poly(alkyl methacrylate) macro-CTAs for the RAFT dispersion polymerization of aromatic methacrylates (e.g. benzyl methacrylate or 3-phenylpropyl methacrylate) in *n*-heptane,[34] *n*-octane,[35] *n*-dodecane,[36] *n*-tetradecane[37] or industrially-relevant solvents such as mineral oil or poly(α-olefins).[38-40] In some cases, such PISA formulations can exhibit interesting thermoresponsive behavior that enables high-temperature oil-thickening.[41] However, there is still significant scope for the synthesis of highly functional nanoparticles in oil.

Glycidyl methacrylate (GlyMA) has proven to be a useful and relatively cheap precursor for the design of highly versatile polymers for post-polymerization modification.[42, 43] Ring-opening reactions involving GlyMA residues and nucleophiles such as water,[44] primary or secondary amines,[45-49] thiols,[50, 51] carboxylic acids,[52] azides[53] and organosilyls[54] have been reported. For example, we recently described the synthesis of well-defined poly(glycerol monomethacrylate)-poly(glycidyl methacrylate) (PGMA-PGlyMA) spherical nanoparticles via RAFT aqueous emulsion polymerization of GlyMA under mild conditions.[55] The epoxy groups located within these PGMA-PGlyMA spheres could be subsequently reacted with sodium azide and diamines were also examined to produce crosslinked nanoparticles. However, the wholly aqueous nature of such formulations inevitably led to relatively poor long-term stability, with the initial linear diblock copolymer chains becoming progressively more branched/crosslinked during their long-term storage at ambient temperature as judged by GPC studies.

Herein we report the PISA synthesis of epoxy-functional poly(stearyl methacrylate)-poly(glycidyl methacrylate) (PSMA-PGlyMA) diblock copolymer nanoparticles via RAFT dispersion polymerization of GlyMA in mineral oil (see Scheme 1). The diblock copolymer chains were characterized by ^{1}H NMR spectroscopy and gel permeation chromatography (GPC),

Department of Chemistry, The University of Sheffield, Dainton Building, Brook Hill, Sheffield, South Yorkshire, S3 7HF, UK. Email: m.derry@sheffield.ac.uk; s.p.armes@sheffield.ac.uk

† Electronic Supplementary Information (ESI) available: Summary table of (co)polymer characterization; Assigned ^{1}H NMR spectra; DLS time study; Reaction scheme for possible chain-branching. See DOI: 10.1039/x0xx00000x

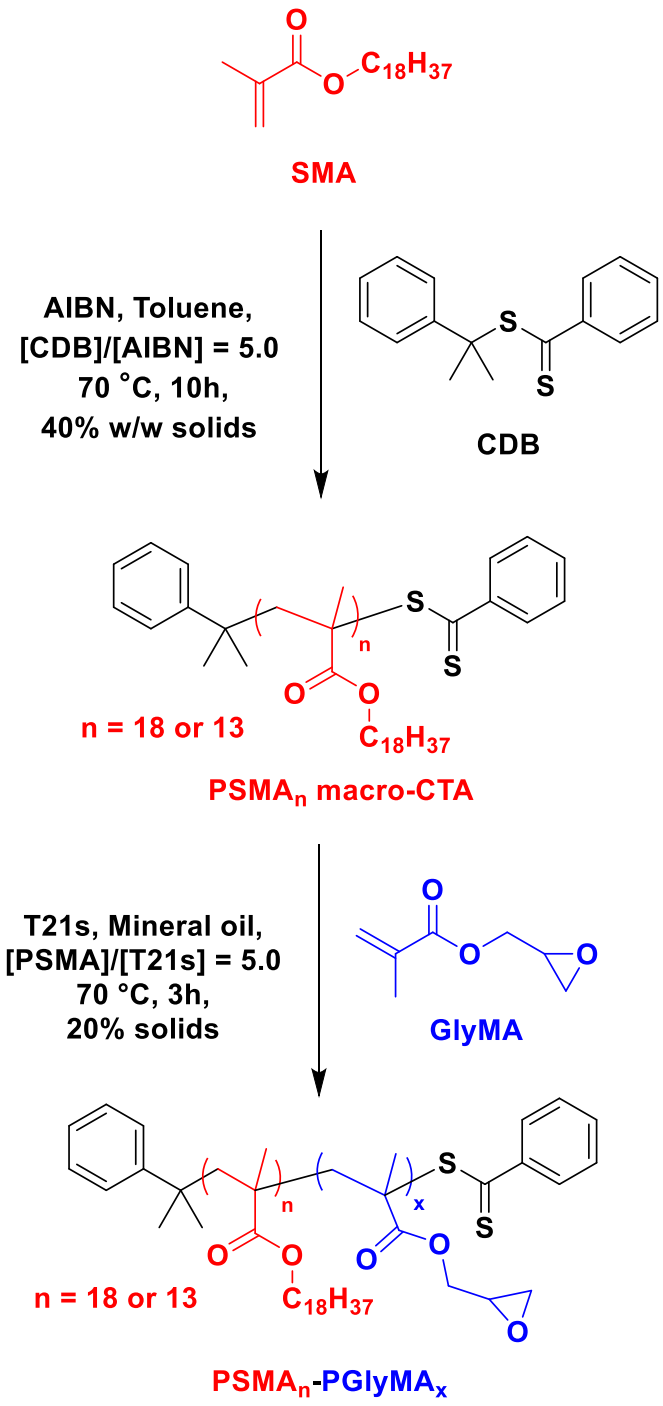

Scheme 1. Synthesis of poly(stearyl methacrylate) (PSMA) macro-CTA via RAFT solution polymerization of stearyl methacrylate (SMA) in toluene using cumyl dithiobenzoate (CDB) at 70 °C, followed by the RAFT dispersion polymerization of glycidyl methacrylate (GlyMA) in mineral oil at 70 °C.

while the nanoparticles were characterized by dynamic light scattering (DLS), FT-IR spectroscopy and transmission electron microscopy (TEM). Particular emphasis was placed on (i) post-polymerization functionalization of such nanoparticles via reaction with a model aromatic amine and (ii) examination of the long-term chemical stability of the reactive epoxide groups within these nanoparticle cores during the long-term storage of such dispersions at ambient temperature.

Experimental

Materials

Glycidyl methacrylate (GlyMA), $CDCl_3$, cumyl dithiobenzoate (CDB) and all other reagents were purchased from Sigma-Aldrich (UK) and were used as received, unless otherwise noted. Stearyl methacrylate (SMA) was purchased from Santa Cruz Biotechnology Ltd. (USA). tert-Butyl peroxy-2-ethylhexanoate (T21s) initiator was purchased from AkzoNobel (The Netherlands). Toluene, $CHCl_3$ and *n*-dodecane were purchased from Fisher Scientific (UK) and CD_2Cl_2 was purchased from Goss Scientific (UK). API Group III mineral oil (viscosity = 3.1 cSt at 100 °C) was provided by The Lubrizol Corporation Ltd (Hazelwood, Derbyshire, UK).

Synthesis of poly(stearyl methacrylate) (PSMA) macro-CTA via RAFT solution polymerization

The synthesis of PSMA macro-CTAs by RAFT solution polymerization has been previously reported.[1] A typical synthesis of a $PSMA_{13}$ macro-CTA at 40% w/w solids was conducted as follows: A 250 mL round-bottomed flask was charged with SMA (26.4 g; 78.0 mmol), CDB (4.25 g; 15.6 mmol; target degree of polymerization = 5), 2,2'-azobisisobutyronitrile (AIBN; 512 mg, 3.12 mmol; CDB/AIBN molar ratio = 5.0) and toluene (46.0 g). The sealed reaction vessel was purged with nitrogen for 30 min, placed in a pre-heated oil bath at 70 °C and stirred for 10 h. The resulting PSMA (PSMA conversion = 85%; M_n = 4,100 g mol^{-1}, M_w/M_n = 1.22) was purified by twice precipitating from toluene into a ten-fold excess of ethanol. The mean degree of polymerization (DP) of this macro-CTA was calculated to be 13 using ^{1}H NMR spectroscopy by comparing the integrated signals corresponding to the ten aromatic protons at 6.8-7.8 ppm with that assigned to the two oxymethylene protons of PSMA at 3.6-4.0 ppm.

Synthesis of poly(stearyl methacrylate)-poly(glycidyl methacrylate) (PSMA-PGlyMA) diblock copolymer nanoparticles via RAFT dispersion polymerization of glycidyl methacrylate in mineral oil

A typical RAFT dispersion polymerization synthesis of $PSMA_{13}$-$PGlyMA_{100}$ diblock copolymer nanoparticles at 20% w/w solids was carried out as follows: GlyMA (0.365 g; 2.57 mmol), T21s initiator (1.11 mg; 5.13 µmol; 10.0% v/v in mineral oil) and $PSMA_{13}$ macro-CTA (0.12 g; 25.7 µmol; macro-CTA/initiator molar ratio = 5.0; target PGlyMA degree of polymerization = 100) were dissolved in mineral oil (1.94 g). The reaction mixture was sealed and purged with nitrogen for 30 min. The deoxygenated solution was placed in a pre-heated oil bath at 70 °C and stirred for 3 h (final GlyMA conversion = 96%; M_n = 16,100 g mol^{-1}, M_w/M_n = 1.19).

Post-polymerization functionalization of PSMA-PGlyMA nanoparticles

N-Methylaniline was added (*N*-methylaniline/GlyMA molar ratio = 1.0) to a 20% w/w dispersion of $PSMA_{13}$-$PGlyMA_{375}$ nanoparticles in mineral oil. This dispersion was stirred at 20 °C, 50 °C or 70 °C until complete reaction of the GlyMA epoxide groups had occurred as judged by ^{1}H NMR spectroscopy. Unreacted *N*-methylaniline was removed via three centrifugation/redispersion cycles at 6,000 rpm (3,421 g) for 99 min, affording functionalized $PSMA_{13}$-$PGlyMA_{375}$ nanoparticles.

Gel Permeation Chromatography (GPC)

Molecular weight distributions (MWDs) were assessed by GPC using a $CHCl_3$ eluent. The GPC set-up comprised two 5 µm (30 cm) Mixed C columns, a HPLC pump and a WellChrom K-2301 refractive index detector operating at 950 ± 30 nm. The mobile phase contained 0.25% v/v triethylamine and the flow rate was fixed at 1.0 mL min^{-1}. A series of twelve near-monodisperse poly(methyl methacrylate) standards (M_p values ranging from 800 to 2,200,000 g mol^{-1}) were used for column calibration.

^{1}H NMR spectroscopy

^{1}H NMR spectra were recorded in either CD_2Cl_2 or $CDCl_3$ using a Bruker AV1-400 MHz spectrometer. Typically, 64 scans were averaged per spectrum. Chemical shifts are expressed in ppm and are internally referenced to the residual solvent peak.

Dynamic Light Scattering (DLS)

DLS studies were performed using a Zetasizer Nano ZS instrument (Malvern Instruments, UK) at a fixed scattering angle of 173°. Copolymer dispersions were diluted in *n*-dodecane (0.10% w/w) prior to light scattering analysis at 25 °C. The intensity-average diameter and polydispersity of the diblock copolymer nanoparticles were calculated by cumulants analysis of the experimental correlation function using Dispersion Technology Software version 6.20. Data were averaged over thirteen runs each of thirty seconds duration.

Fourier Transform Infrared (FT-IR) spectroscopy

FT-IR spectra were recorded on 20% w/w diblock copolymer dispersions at room temperature (124 scans accumulated per spectrum) using a Thermo-Scientific Nicolet IS10 FT-IR spectrometer equipped with a Golden Gate Diamond ATR accessory.

Transmission Electron Microscopy (TEM)

TEM studies were conducted using a Philips CM 100 instrument operating at 100 kV and equipped with a Gatan 1 k CCD camera. Diluted diblock copolymer dispersions (0.10% w/w) were placed on carbon-coated copper grids and exposed to ruthenium(VIII) oxide vapor for 7 min at 20 °C prior to analysis.[2] This heavy metal compound acted as a positive stain for the core-forming PGlyMA block to improve contrast. The ruthenium(VIII) oxide was prepared as follows: ruthenium(IV) oxide (0.30 g) was added to water (50 g) to form a black slurry; addition of sodium periodate (2.0 g) with continuous stirring produced a yellow solution of ruthenium(VIII) oxide within 1 min.[3]

Purification of functionalized PSMA-PGlyMA spheres

Centrifugation was performed using a Heraeus Biofuge Pico centrifuge at 6,000 rpm (3,421 g) for 99 min until clear supernatants were observed. The supernatants were carefully decanted and the sedimented nanoparticles were redispersed in fresh mineral oil for further centrifugation/redispersion cycles.

Results and Discussion

Synthesis of PSMA macro-CTAs

A PSMA macro-CTA was preferred as the stabilizer block instead of poly(lauryl methacrylate) (PLMA), which had been utilized for the first all-methacrylic non-polar PISA formulation.[34] This is because PSMA macro-CTAs exhibit significantly enhanced pseudo-living character during dispersion polymerizations, although the reason(s) for such behavior are not fully understood.[39] The $PSMA_{18}$ macro-CTA utilized was synthesized as previously reported.[39] The $PSMA_{13}$ macro-CTA was synthesized using the same method (via RAFT solution polymerization of SMA in toluene at 70 °C using CDB as a RAFT CTA, see Scheme 1). The SMA polymerization was quenched by exposure to air once 85% monomer conversion was achieved, thus avoiding monomer-starved conditions. Previously reported kinetics were utilized in order to ensure this desired monomer conversion.[39] Both PSMA macro-CTAs possessed narrow molecular weight distributions ($M_w/M_n \leq 1.22$), indicating that good control was during the RAFT solution polymerization of SMA. Moreover, this synthetic protocol also led to high RAFT end-group fidelity, which enabled a relatively high blocking efficiency to be achieved on addition of the GlyMA monomer (see below). This is essential for the synthesis of well-defined diblock copolymers.

RAFT dispersion polymerization of GlyMA in mineral oil

Representative kinetic data obtained for the RAFT dispersion polymerization of GlyMA in mineral oil at 70 °C and 20% w/w solids was conducted when targeting $PSMA_{18}$-$PGlyMA_{100}$ nanoparticles (see Figure 1). Aliquots from the polymerizing reaction solution were taken at 10 min intervals for the first hour, followed by 20 min intervals for the second hour and then every 30 min thereafter. The GlyMA polymerization proceeded relatively slowly for the first 40 min, after which an approximate eight-fold rate increase was observed. This rate enhancement is well-known for PISA syntheses and is attributed to micellar nucleation. Nascent nanoparticles are formed when the growing core-forming chains eventually become insoluble, then unreacted monomer diffuses into the nanoparticle cores and thus provides a significantly higher local monomer concentration.[38, 56] The kinetic data shown in

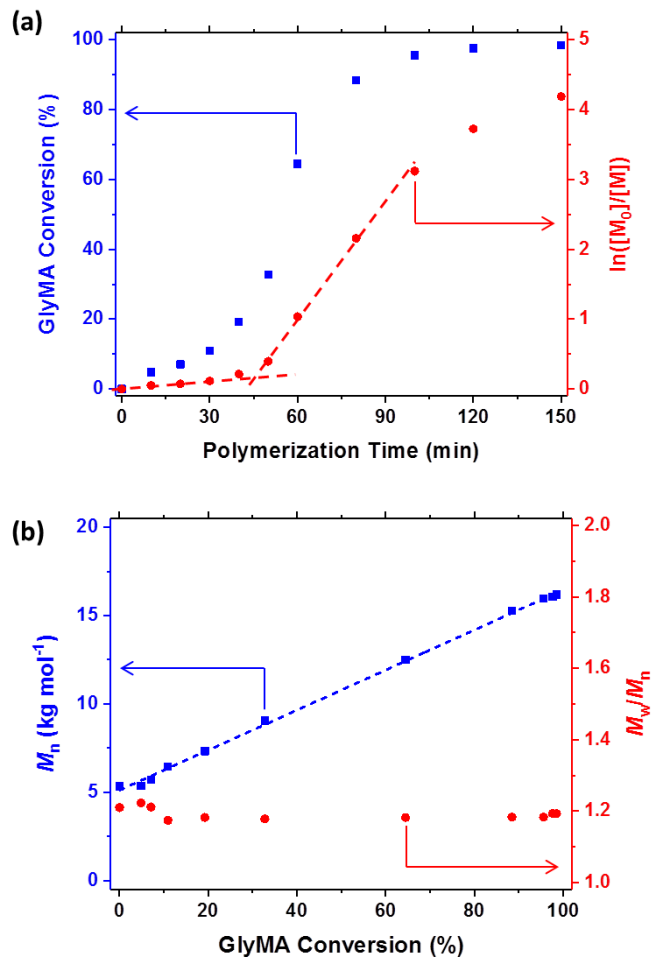

Figure 1. (a) GlyMA monomer conversion vs. polymerization time (blue squares) and ln([M]$_0$/[M]) vs. polymerization time (red circles) and (b) M_n vs. GlyMA conversion (blue squares) and M_w/M_n vs. GlyMA conversion (red circles) during the synthesis of PSMA$_{18}$-PGlyMA$_{100}$ nanoparticles via RAFT dispersion polymerization of GlyMA at 20% w/w solids in mineral oil at 70 °C.

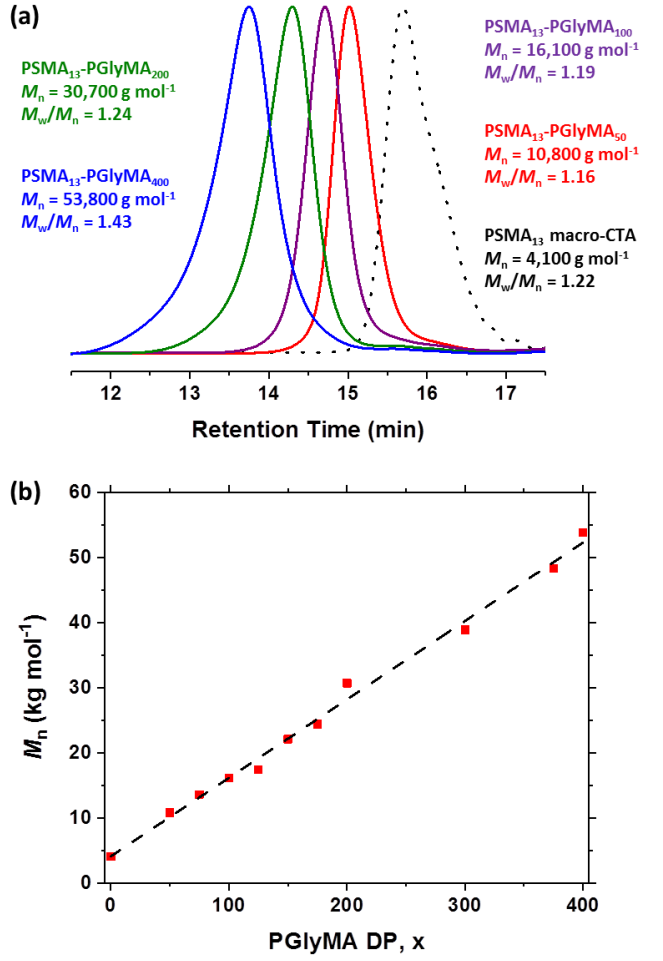

Figure 2. (a) $CHCl_3$ gel permeation chromatograms (vs. poly(methyl methacrylate) standards) obtained for six PSMA$_{13}$-PGlyMA$_x$ diblock copolymers prepared via RAFT dispersion polymerization of glycidyl methacrylate in mineral oil at 70 °C at 20% w/w solids. The precursor PSMA$_{13}$ macro-CTA (prepared in toluene at 70 °C at 40% w/w solids) is also shown as a reference (black dashed curve). (b) M_n vs. PGlyMA DP for the series of PSMA$_{13}$-PGlyMA$_x$ diblock copolymers.

Figure 1 suggest that the critical copolymer composition at which nanoparticles are first formed corresponds to PSMA$_{13}$-PGlyMA$_{25}$ (or 25% GlyMA conversion). First-order kinetics were observed from 25% to 90% monomer conversion, after which monomer-starved conditions led to a reduction in the rate of polymerization. More than 99% GlyMA conversion was achieved within 150 min at 70 °C. Good control over this polymerization was confirmed by GPC analysis, which revealed a linear relationship between M_n and monomer conversion and relatively narrow molecular weight distributions (M_w/M_n < 1.22), see Figure 1b.

Two series of PSMA-PGlyMA nanoparticles were synthesized via RAFT dispersion polymerization at 70 °C using either the PSMA$_{13}$ or PSMA$_{18}$ macro-CTA at 20% w/w solids in mineral oil. At least 94% GlyMA conversion was achieved within 3 h in all cases, as confirmed by ^{1}H NMR spectroscopy (see Table S1). GPC analyses indicated that, in general, reasonably good RAFT control (M_w/M_n < 1.30) was achieved when targeting PGlyMA DPs up to 200 using either PSMA macro-CTA. However, a systematic loss in control was observed when targeting higher PGlyMA DPs, which has been reported for related RAFT dispersion polymerization syntheses conducted in non-polar media.[39] Nevertheless, a linear relationship between M_n and GlyMA conversion is obtained despite this gradual broadening of the molecular weight distribution (see Figure 2b). Moreover, the unimodal nature of the chromatograms and a clear shift to higher molecular weight compared to the PSMA macro-CTA suggests that relatively high blocking efficiencies were achieved (see Figure 2a).

PSMA$_{18}$-PGlyMA$_x$ and PSMA$_{13}$-PGlyMA$_x$ diblock copolymer spheres

For both series of PSMA$_{18}$-PGlyMA$_x$ and PSMA$_{13}$-PGlyMA$_x$ diblock copolymers, only spherical nanoparticles were produced as determined by TEM and DLS analyses (see Figure 3). This indicates that the steric stabilization conferred by these relatively short PSMA stabilizer blocks was sufficient to prevent the 1D fusion of multiple spheres, which is a

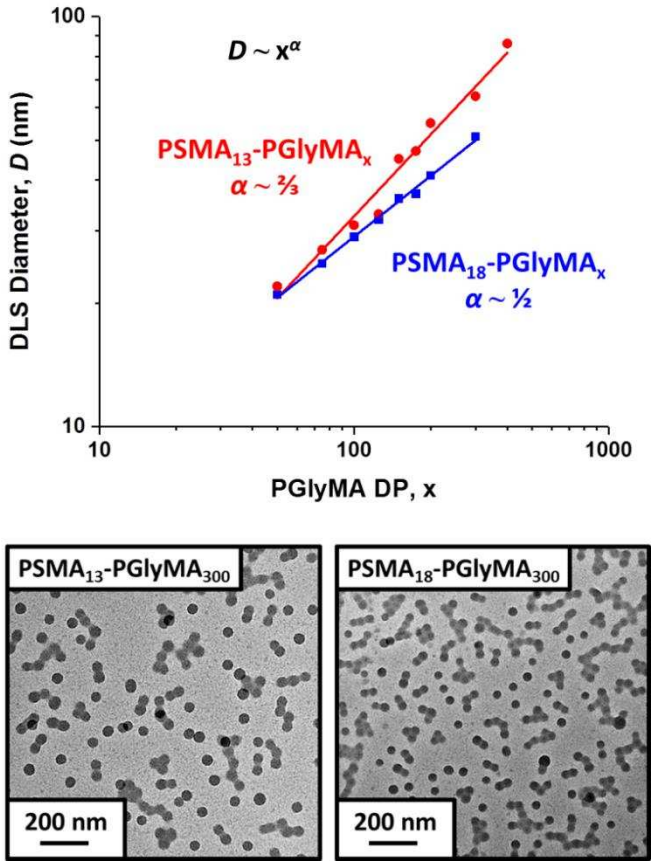

Figure 3. DLS diameter (*D*) vs. target PGlyMA DP (x) for series of $PSMA_{18}$–$PGlyMA_x$ (red circles) and $PSMA_{13}$–$PGlyMA_x$ (blue squares) diblock copolymer spheres prepared via RAFT dispersion polymerization of GlyMA in mineral oil at 70 °C and 20% w/w (top). Transmission electron micrographs for $PSMA_{18}$-$PGlyMA_{150}$ and $PSMA_{13}$-$PGlyMA_{150}$ nanoparticles obtained for 0.10% w/w dispersions in *n*-dodecane.

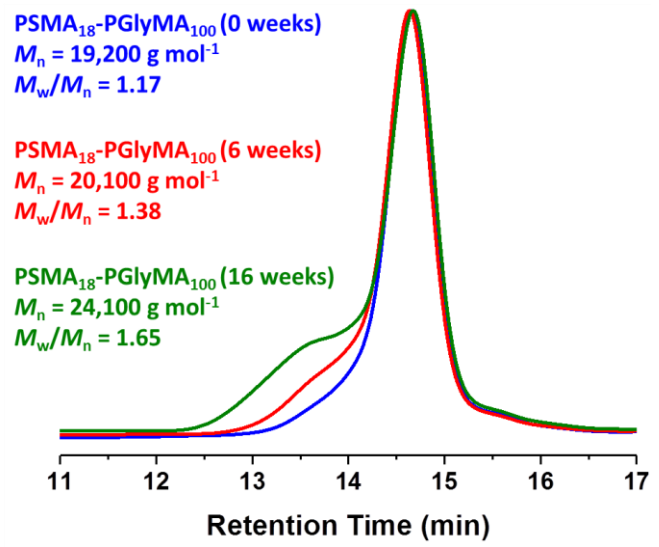

Figure 4. Gel permeation chromatograms recorded for $PSMA_{18}$-$PGlyMA_{100}$ immediately after synthesis (blue data), after 6 weeks (red data) and after 16 weeks (green data). The gradual appearance of a high molecular weight shoulder indicates intermolecular ring-opening side-reactions that lead to light branching.

prerequisite to the formation of higher order morphologies such as worms or vesicles.[8] Nevertheless, the spheres were well-defined and their mean diameter could be readily tuned simply by varying the target DP of the core-forming PGlyMA block. For example, $PSMA_{18}$-$PGlyMA_x$ spheres ranging from 21 nm to 51 nm diameter (as judged by DLS) were obtained when targeting x values of 50 to 300. In comparison, diameters of 22 nm to 86 nm were obtained for $PSMA_{13}$-$PGlyMA_x$ spheres when targeting x values of 50 to 400. Such monotonic increases in particle size as the mean DP of the core-forming block was systematically increased were confirmed by TEM studies. The mean spherical diameter, *D*, is related to the mean DP of the core-forming block, x, by a scaling component, α, such that $D \sim x^{\alpha}$.[57, 58] This relationship is best demonstrated by a plot of log *D* (as determined by DLS) against log x for each series of $PSMA_{18}$-$PGlyMA_x$ and $PSMA_{13}$-$PGlyMA_x$ spheres (see Figure 3). Thus, the scaling component, α, can be determined in each case, which provides valuable information regarding the physical nature of the core-forming PGlyMA chains within the spheres. The $PSMA_{18}$-$PGlyMA_x$ series returned an α value of approximately 0.50, which corresponds to the weak segregation limit and thus relatively unperturbed PGlyMA chains.

However, the $PSMA_{13}$-$PGlyMA_x$ series exhibited a somewhat larger α value of around 0.67. This indicates the strong segregation regime and suggests that the PGlyMA chains adopt a more stretched conformation within the nanoparticle cores in this case.[57, 58] As a consequence, when targeting a given PGlyMA DP, larger spheres are invariably produced when using the shorter $PSMA_{13}$ stabilizer block. For example, a mean DLS diameter *D* of 55 nm was obtained when targeting a $PSMA_{13}$-$PGlyMA_{200}$ spheres compared to $PSMA_{18}$-$PGlyMA_{200}$ spheres (*D* = 41 nm).

Long-term stability of epoxy functionality for non-polar dispersions of $PSMA_{18}$-$PGlyMA_{100}$ spheres stored at 20 °C

Comparison of the ^{1}H NMR signals corresponding to the oxymethylene and epoxy protons within GlyMA residues confirmed that essentially all of the pendent epoxide groups survived intact during the PISA synthesis (see Figure S1). To assess the long-term stability of these reactive epoxy groups, a 20% w/w dispersion of $PSMA_{18}$-$PGlyMA_{100}$ spheres was stored at 20 °C and periodically analyzed via ^{1}H NMR spectroscopy and GPC over 16 weeks. During this period, a 9% reduction in epoxide groups was observed by ^{1}H NMR spectroscopy (see Figure S2). However, this is significantly better than the relatively poor epoxide stability exhibited by GlyMA-based nanoparticles prepared in aqueous media, where a 27% reduction in epoxy content was observed after 12 weeks.[55]

Despite only a relatively modest 9% reduction in epoxy functionality, the effect of ring-opening such highly-strained groups is clearly evidenced by GPC analysis. A high molecular weight shoulder evolves over time, resulting in an increase in both M_n (from 19,200 g mol^{-1} to 24,100 g mol^{-1}) and M_w/M_n (from 1.17 to 1.65), see Figure 4. This is most likely the result of a minor proportion of the epoxides undergoing ring-opening with trace water to form a *cis*-diol species,[59] which can

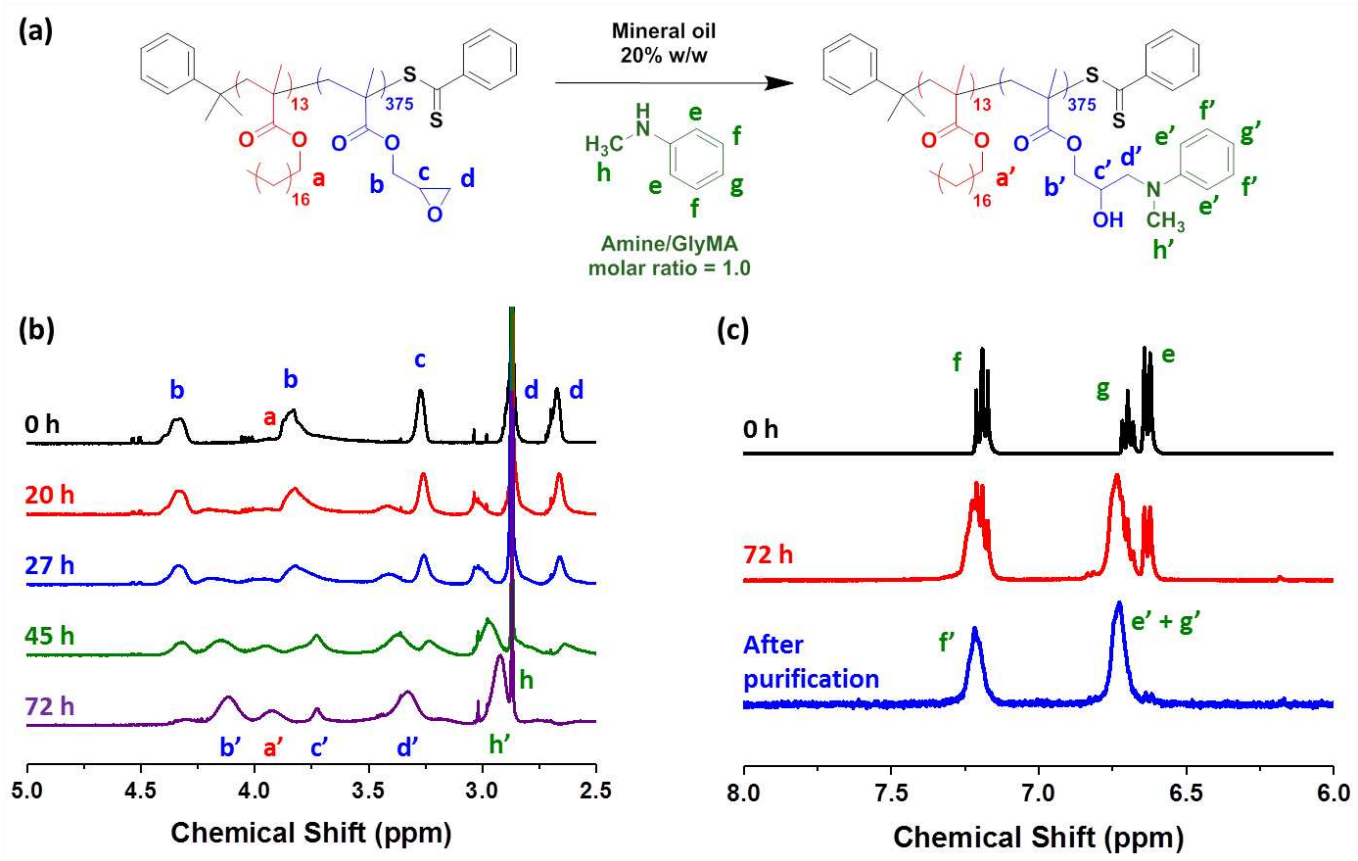

Figure 5. (a) Post-polymerization functionalization of $PSMA_{13}$-$PGlyMA_{375}$ nanoparticles with *N*-methylaniline. (b) Assigned partial ^1H NMR spectra ($CDCl_3$) showing the reduction in epoxide peaks during the reaction of *N*-methylaniline with a 20% w/w dispersion of $PSMA_{13}$-$PGlyMA_{375}$ nanoparticles at 50 °C. (c) Assigned partial ^1H NMR spectra for the transformation of monomeric *N*-methylaniline aromatic peaks into polymeric peaks.

subsequently react with neighboring epoxy groups on adjacent chains and result in light branching. It is therefore proposed that similar side-reactions are also the cause of the poorer epoxy retention observed for aqueous dispersions. Indeed, GPC analysis of an aqueous dispersion of $PGMA_{45}$-$PGlyMA_{100}$ spherical nanoparticles indicated the appearance of a prominent high molecular weight shoulder after 12 weeks, with M_n increasing from 31,200 g mol^{-1} to 46,700 g mol^{-1} and M_w/M_n increasing from 1.24 to 1.63.[55] Additionally, DLS studies confirm that the spherical nanoparticles remain essentially unchanged (see Figure S3).

Post-polymerization functionalization of $PSMA_{13}$-$PGlyMA_{375}$ spheres

To demonstrate the potential for post-polymerization functionalization of these nanoparticles, *N*-methylaniline was added to a stirred 20% w/w dispersion of 99 nm $PSMA_{13}$-$PGlyMA_{375}$ spheres at an amine/GlyMA molar ratio of unity (see Figure 5a). Relatively large spheres were selected for such model reactions because they can be readily sedimented via centrifugation to assess the amount of unreacted *N*-methylaniline remaining in the supernatant. Moreover, GPC analysis of these copolymer chains indicated reasonably good control over the RAFT dispersion polymerization (M_n = 48,300 g mol^{-1}; M_w/M_n = 1.31). Initial experiments were conducted at 20 °C, 50 °C and 70 °C. Shortly after addition of the nucleophilic amine, the dispersion changed from pink to white, suggesting loss of the RAFT end-groups. This was not unexpected, because it is well-known that nucleophiles can react with dithiobenzoates to yield thiol-terminated polymer chains.[60] However, such loss of chain-ends is not detrimental in this case as no further chain extension is required. Indeed, facile RAFT chain-end removal from nanoparticles may be advantageous for potential applications in which the intrinsic color associated with the RAFT chain-ends is not desired. During the epoxy-amine reaction, aliquots were taken periodically to determine the extent of functionalization via ^1H NMR spectroscopy. Complete loss of epoxy signals was observed within 18 h at 70 °C and within 72 h at 50 °C (see Figure 5b). In contrast, only 23% of the epoxide groups had reacted within 72 h at 20 °C. The loss of epoxide groups was coupled with a shift in (and concomitant broadening of) the initially sharp aromatic signals corresponding to *N*-methylaniline (see Figure 5c), which suggested that this functionality was incorporated into the copolymer chains. For the epoxy-amine reaction conducted at 50 °C, the extent of functionalization was determined to be 78% by comparing the integrals of the sharp monomeric doublet at 6.63 ppm

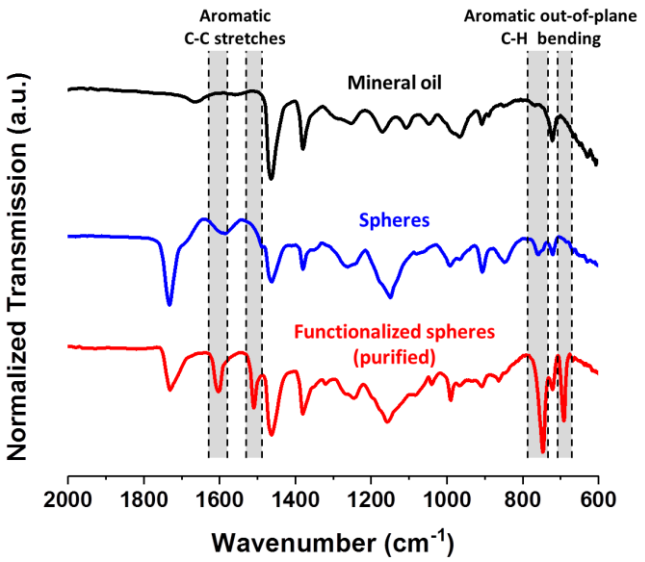

Figure 6. FT-IR spectra recorded for mineral oil (black data, top), 20% w/w dispersion of $PSMA_{13}$-$PGlyMA_{375}$ spheres prior to functionalization (blue data, middle) and 20% w/w dispersion of $PSMA_{13}$-$PGlyMA_{375}$ spheres after functionalization with *N*-methylaniline and subsequent purification (red data, bottom).

(corresponding to the two *ortho* protons in the unreacted *N*-methylaniline) with that at 6.70 ppm (corresponding to polymeric *ortho* and *para* protons and residual monomeric *para* proton). Clearly, complete loss of the epoxy signals does not correspond to full reaction of the *N*-methylaniline. This is presumably because the hydroxyl group generated during ring-opening of each epoxide can potentially react with other epoxide groups, either intramolecularly or intermolecularly (Scheme S1). Evidence for such intermolecular reactions was provided by GPC analysis, which revealed higher M_n and M_w/M_n values and also the appearance of a high molecular weight shoulder (see Figure 4). However, the extent of such side-reactions was insufficient to fully crosslink the PGlyMA cores as evidenced by complete dissolution of the nanoparticles in a common solvent for both blocks ($CHCl_3$). Nevertheless, most of the unreacted *N*-methylaniline was removed via three centrifugation-redispersion cycles, as confirmed by the almost complete disappearance of the monomeric aromatic proton signals in the resulting ^{1}H NMR spectrum (see Figure 5c). In fact, only 6% unreacted *N*-methylaniline remained after purification. It is well-known that aromatic amines such as *para*-phenylenediamine derivatives can act as anti-knock agents[61] or anti-oxidants.[62] In principle, covalent grafting of such small molecules to oil-dispersible nanoparticles may enable their effective concentration to be increased in fuels and lubricating oils. This approach could add considerable value to spherical diblock copolymer nanoparticles dispersed in base oil, which have already been shown to provide enhanced friction reduction.[63]

FT-IR spectroscopy was also performed to confirm the functionalization. Distinctive new bands were observed on the reaction of *N*-methylaniline with the PSMA-PGlyMA spheres: an aromatic C-C stretches at ~1510 cm^{-1} and ~1600 cm^{-1}, and out-of-plane aromatic C-H bending at ~690 cm^{-1} and ~730 cm^{-1} are observed after purification via centrifugation (see Figure 6).

On reaction of PSMA-PGlyMA spheres with primary amines (e.g. aniline or benzylamine) or diamines (e.g. ethylene diamine), GPC analyses in $CHCl_3$ were no longer possible. Extensive crosslinking of the nanoparticle cores was confirmed by DLS studies performed in $CHCl_3$: nanoparticles remained intact when redispersed in this solvent, whereas immediate dissolution was observed for the precursor linear nanoparticles. In principle, this crosslinking chemistry may enhance the mechanical properties of such spheres.

Conclusions

In summary, a series of PSMA-PGlyMA nanoparticles were synthesized via RAFT dispersion polymerization of GlyMA at 70 °C in mineral oil at 20% w/w solids. Good control over the polymerization was achieved when using both $PSMA_{18}$ and $PSMA_{13}$ macro-CTAs as judged by GPC analysis. The mean diameter of the resulting PSMA-PGlyMA spheres was tunable simply varying the core-forming PGlyMA DP, with $PSMA_{13}$-$PGlyMA_x$ spheres being invariably larger than $PSMA_{18}$-$PGlyMA_x$ spheres for given values of x. Importantly, the long-term stability of the epoxy functionality within such nanoparticles proved to be much better than that for a related aqueous PISA formulation, with only a 9% reduction in epoxy functionality being observed after 16 weeks storage at 20 °C. In principle, these epoxy groups enable facile modification of such nanoparticles, as exemplified by the reaction of $PSMA_{18}$-$PGlyMA_{375}$ spheres with *N*-methylaniline. On heating to 50 °C, ring-opening of the epoxy groups was complete within 72 h and 78% functionalization could be achieved with *N*-methylaniline. Three centrifugation-redispersion cycles were sufficient to ensure removal of unreacted *N*-methylaniline and ^{1}H NMR and FT-IR spectroscopy studies confirmed successful derivatization of $PSMA_{18}$-$PGlyMA_{375}$ spheres. Importantly, well-defined (albeit larger) spheres were obtained after this epoxy-amine derivatization. In principle, this new route to functional block copolymer nanoparticles dispersed in mineral oil should provide opportunities for the rational design of next-generation engine oil additives.

Conflicts of interest

There are no conflicts to declare.

Acknowledgements

S.P.A. acknowledges an EPSRC Established Career Fellowship (EP/R003009/1). The Leverhulme Trust is also thanked for post-doctoral support of M.J.D. (RPG-2016-330). Dr. Svetomir Tzokov at The University of Sheffield Biomedical Science Electron Microscopy Suite is thanked for TEM assistance. The Lubrizol Corporation (Hazelwood, UK) is thanked for supplying the mineral oil used in this work.

References

1. J. Chiefari, Y. K. Chong, F. Ercole, J. Krstina, J. Jeffery, T. P. T. Le, R. T. A. Mayadunne, G. F. Meijs, C. L. Moad, G. Moad, E. Rizzardo and S. H. Thang, *Macromolecules*, 1998, **31**, 5559-5562.
2. G. Moad, E. Rizzardo and S. H. Thang, *Australian Journal of Chemistry*, 2009, **62**, 1402-1472.
3. S. Perrier, *Macromolecules*, 2017, **50**, 7433-7447.
4. B. D. Fairbanks, P. A. Gunatillake and L. Meagher, *Advanced Drug Delivery Reviews*, 2015, **91**, 141-152.
5. M. Haeussler, J. Chiefari, G. Moad and E. Rizzardo, in *Polymers for Personal Care and Cosmetics*, American Chemical Society, 2013, vol. 1148, ch. 10, pp. 157-172.
6. A. J. Brzytwa and J. Johnson, *Polymer Preprints (American Chemical Society, Division of Polymer Chemistry)*, 2011, **52**, 533-534.
7. N. J. Warren and S. P. Armes, *Journal of the American Chemical Society*, 2014, **136**, 10174-10185.
8. M. J. Derry, L. A. Fielding and S. P. Armes, *Progress in Polymer Science*, 2016, **52**, 1-18.
9. S. L. Canning, G. N. Smith and S. P. Armes, *Macromolecules*, 2016, **49**, 1985-2001.
10. Y. Pei, A. B. Lowe and P. J. Roth, *Macromolecular Rapid Communications*, 2017, **38**, 1600528.
11. J. Rieger, C. Grazon, B. Charleux, D. Alaimo and C. Jérôme, *Journal of Polymer Science Part A: Polymer Chemistry*, 2009, **47**, 2373-2390.
12. X. Zhang, S. Boisse, W. Zhang, P. Beaunier, F. D'Agosto, J. Rieger and B. Charleux, *Macromolecules*, 2011, **44**, 4149-4158.
13. W. Zhang, B. Charleux and P. Cassagnau, *Macromolecules*, 2012, **45**, 5273-5280.
14. W. J. Zhang, F. D'Agosto, O. Boyron, J. Rieger and B. Charleux, *Macromolecules*, 2012, **45**, 4075-4084.
15. W. Zhang, F. D'Agosto, P.-Y. Dugas, J. Rieger and B. Charleux, *Polymer*, 2013, **54**, 2011-2019.
16. A. A. Cockram, T. J. Neal, M. J. Derry, O. O. Mykhaylyk, N. S. J. Williams, M. W. Murray, S. N. Emmett and S. P. Armes, *Macromolecules*, 2017, **50**, 796-802.
17. R. Deng, M. J. Derry, C. J. Mable, Y. Ning and S. P. Armes, *Journal of the American Chemical Society*, 2017, **139**, 7616-7623.
18. W. Cai, W. Wan, C. Hong, C. Huang and C. Pan, *Soft Matter*, 2010, **6**, 5554-5561.
19. C.-Q. Huang and C.-Y. Pan, *Polymer*, 2010, **51**, 5115-5121.
20. W.-D. He, X.-L. Sun, W.-M. Wan and C.-Y. Pan, *Macromolecules*, 2011, **44**, 3358-3365.
21. C.-Q. Huang, Y. Wang, C.-Y. Hong and C.-Y. Pan, *Macromolecular Rapid Communications*, 2011, **32**, 1174-1179.
22. M. Semsarilar, E. R. Jones, A. Blanazs and S. P. Armes, *Advanced Materials*, 2012, **24**, 3378-3382.
23. Y. Pei and A. B. Lowe, *Polymer Chemistry*, 2014, **5**, 2342-2351.
24. Y. W. Pei, N. C. Dharsana, J. A. Van Hensbergen, R. P. Burford, P. J. Roth and A. B. Lowe, *Soft Matter*, 2014, **10**, 5787-5796.
25. W.-J. Zhang, C.-Y. Hong and C.-Y. Pan, *Macromolecular Rapid Communications*, 2015, **36**, 1428-1436.
26. Y. Pei, N. C. Dharsana and A. B. Lowe, *Australian Journal of Chemistry*, 2015, **68**, 939-945.
27. Y. W. Pei, J. M. Noy, P. J. Roth and A. B. Lowe, *Polymer Chemistry*, 2015, **6**, 1928-1931.
28. E. R. Jones, O. O. Mykhaylyk, M. Semsarilar, M. Boerakker, P. Wyman and S. P. Armes, *Macromolecules*, 2016, **49**, 172-181.
29. L. Houillot, C. Bui, M. Save, B. Charleux, C. Farcet, C. Moire, J.-A. Raust and I. Rodriguez, *Macromolecules*, 2007, **40**, 6500-6509.
30. L. Houillot, C. Bui, C. Farcet, C. Moire, J.-A. Raust, H. Pasch, M. Save and B. Charleux, *ACS Applied Materials & Interfaces*, 2010, **2**, 434-442.
31. A. P. Lopez-Oliva, N. J. Warren, A. Rajkumar, O. O. Mykhaylyk, M. J. Derry, K. E. B. Doncom, M. J. Rymaruk and S. P. Armes, *Macromolecules*, 2015, **48**, 3547-3555.
32. Y. Pei, J.-M. Noy, P. J. Roth and A. B. Lowe, *Journal of Polymer Science Part A: Polymer Chemistry*, 2015, **53**, 2326-2335.
33. M. J. Rymaruk, K. L. Thompson, M. J. Derry, N. J. Warren, L. P. D. Ratcliffe, C. N. Williams, S. L. Brown and S. P. Armes, *Nanoscale*, 2016, **8**, 14497-14506.
34. L. A. Fielding, M. J. Derry, V. Ladmiral, J. Rosselgong, A. M. Rodrigues, L. P. D. Ratcliffe, S. Sugihara and S. P. Armes, *Chemical Science*, 2013, **4**, 2081-2087.
35. Y. Pei, O. R. Sugita, L. Thurairajah and A. B. Lowe, *RSC Advances*, 2015, **5**, 17636-17646.
36. L. A. Fielding, J. A. Lane, M. J. Derry, O. O. Mykhaylyk and S. P. Armes, *Journal of the American Chemical Society*, 2014, **136**, 5790-5798.
37. Y. Pei, L. Thurairajah, O. R. Sugita and A. B. Lowe, *Macromolecules*, 2015, **48**, 236-244.
38. M. J. Derry, L. A. Fielding and S. P. Armes, *Polymer Chemistry*, 2015, **6**, 3054-3062.
39. M. J. Derry, L. A. Fielding, N. J. Warren, C. J. Mable, A. J. Smith, O. O. Mykhaylyk and S. P. Armes, *Chemical Science*, 2016, **7**, 5078-5090.
40. M. J. Derry, O. O. Mykhaylyk, A. J. Ryan and S. P. Armes, *Chemical Science*, 2018, **9**, 4071-4082.
41. M. J. Derry, O. O. Mykhaylyk and S. P. Armes, *Angewandte Chemie International Edition*, 2017, **56**, 1746-1750.
42. M. Benaglia, A. Alberti, L. Giorgini, F. Magnoni and S. Tozzi, *Polymer Chemistry*, 2013, **4**, 124-132.
43. Ezzah M. Muzammil, A. Khan and M. C. Stuparu, *RSC Advances*, 2017, **7**, 55874-55884.
44. M.-C. Jones, P. Tewari, C. Blei, K. Hales, D. J. Pochan and J.-C. Leroux, *Journal of the American Chemical Society*, 2006, **128**, 14599-14605.
45. H. Gao, M. Elsabahy, E. V. Giger, D. Li, R. E. Prud'homme and J.-C. Leroux, *Biomacromolecules*, 2010, **11**, 889-895.
46. F. J. Xu, M. Y. Chai, W. B. Li, Y. Ping, G. P. Tang, W. T. Yang, J. Ma and F. S. Liu, *Biomacromolecules*, 2010, **11**, 1437-1442.
47. H. Gao, X. Lu, Y. Ma, Y. Yang, J. Li, G. Wu, Y. Wang, Y. Fan and J. Ma, *Soft Matter*, 2011, **7**, 9239-9247.
48. F. J. Xu, Y. Zhu, M. Y. Chai and F. S. Liu, *Acta Biomaterialia*, 2011, **7**, 3131-3140.
49. O. I. Strube, N. Lars, A. Zaure and S.-N. Gudrun, *Macromol. Chem. Phys.*, 2012, **213**, 1274-1284.
50. S. De and A. Khan, *Chemical Communications*, 2012, **48**, 3130-3132.
51. C. György, J. R. Lovett, N. J. W. Penfold and S. P. Armes, *Macromolecular Rapid Communications*, 2018, DOI: 10.1002/marc.201800289.
52. V. Tsyalkovsky, V. Klep, K. Ramaratnam, R. Lupitskyy, S. Minko and I. Luzinov, *Chemistry of Materials*, 2008, **20**, 317-325.
53. N. V. Tsarevsky, S. A. Bencherif and K. Matyjaszewski, *Macromolecules*, 2007, **40**, 4439-4445.
54. K. D. Safa and M. H. Nasirtabrizi, *Polym. Bull.*, 2006, **57**, 293-304.
55. F. L. Hatton, J. R. Lovett and S. P. Armes, *Polymer Chemistry*, 2017, **8**, 4856-4868.
56. A. Blanazs, J. Madsen, G. Battaglia, A. J. Ryan and S. P. Armes, *Journal of the American Chemical Society*, 2011, **133**, 16581-16587.

57. F. S. Bates and G. H. Fredrickson, *Annual Review of Physical Chemistry*, 1990, **41**, 525-557.
58. S. Förster, M. Zisenis, E. Wenz and M. Antonietti, *Journal of Chemical Physics*, 1996, **104**, 9956-9970.
59. L. P. D. Ratcliffe, A. J. Ryan and S. P. Armes, *Macromolecules*, 2013, **46**, 769-777.
60. H. Willcock and R. K. O'Reilly, *Polymer Chemistry*, 2010, **1**, 149-157.
61. J. E. Brown, F. X. Markley and H. Shapiro, *Industrial & Engineering Chemistry*, 1955, **47**, 2141-2146.
62. K. Varatharajan, M. Cheralathan and R. Velraj, *Fuel*, 2011, **90**, 2721-2725.
63. R. Zheng, G. Liu, M. Devlin, K. Hux and T.-C. Jao, *Tribology Transactions*, 2010, **53**, 97-107.